0270-6474/82/0209-1267$02.00/0

The Journal of Neuroscience
Vol. 2, No. 9, pp. 1267–1274
September 1982

ULTRASTRUCTURAL FEATURES OF IMMUNOREACTIVE SOMATOSTATIN NEURONS IN THE RAT CAUDATE NUCLEUS[1]

MARIAN DiFIGLIA[2] AND NEIL ARONIN

Department of Neurology, Massachusetts General Hospital and Harvard Medical School, Boston Massachusetts 02114 and the Departments of Medicine and Physiology, University of Massachusetts School of Medicine, Worcester, Massachusetts 01605

Received February 24, 1982; Revised April 19, 1982; Accepted April 20, 1982

Abstract

Previous immunocytochemical studies have localized immunoreactive (i) somatostatin (SS) to cell bodies and fibers in the rat neostriatum. In order to identify the population of neostriatal neurons that contain iSS, we used the immunoperoxidase technique to study the localization of iSS at both the light and electron microscopic levels. Light microscopic results showed that iSS was present within small to medium size cell bodies (9 to 20 μm in size) and their emerging processes which were visible for long distances (up to 120 μm) away from the somata. Dendrites were of different diameters, branched into secondary and tertiary processes, and exhibited smooth or irregular contours. Dendrites contained prominent swellings, particularly at branch points, and gave rise to fine beaded processes. At the ultrastructural level, iSS neurons contained deeply indented nuclei and a relatively rich cytoplasm, including well developed Golgi apparatus and rough endoplasmic reticulum which was organized into small stacks. Proximal and distal dendrites had an irregular or varicose appearance, rarely exhibited spines, and were contacted by at least two types of unlabeled axon terminals. Immunoreactive SS also was present in myelinated axons (0.2 to 0.5 μm) which were observed in bundles of internal capsule fibers and in small diameter unmyelinated axons (0.1 to 0.2 μm). The latter coursed through the caudate neuropil and gave rise to swellings which made synapses *en passant*. Somatostatin-containing axon terminals were about 0.5 μm in size, contained numerous clear pleomorphic and few large granular vesicles, and made synaptic contact with dendrites and dendritic spines.

The morphologic features of iSS neurons closely correspond to the category of medium size aspiny neurons which have been recognized in Golgi studies and in electron microcospic studies of Golgi-impregnated and intracellular horseradish peroxidase-labeled neurons, and they differ from those of medium size spiny neurons identified by similar Golgi-electron microscopic methods. It is likely that many of the iSS fibers and boutons observed in the caudate originate from intrinsic cells. However, extrinsic sources of somatostatin also may exist.

Somatostatin (SS), a tetradecapeptide, has been demonstrated by radioimmunoassay (Brownstein et al., 1975; Kobayashi et al., 1977) and immunohistochemistry (Krisch, 1978; Bennett-Clark et al., 1980; Finley et al., 1981) to have a wide distribution within the central nervous system, including the basal ganglia. Fibers and cell bodies containing immunoreactive (i) SS have been observed in the rat neostriatum at the light microscopic level (Elde et al., 1978; Krisch and Leonhardt, 1980). To date, there are no reports on the ultrastructure of neostriatal iSS neurons or the possible cell type to which

[1] This work was supported in part by National Institutes of Health Grants NS 16367 (M. D.) and AM 01126-01 (N. A.), the Hereditary Disease Foundation (M. D.), and University of Massachusetts Medical Center Institutional Biomedical Research Support Grant 2S-07RR05712-10 (N. A.). We wish to thank Ms. Jan Carey and Ms. Kathleen Sullivan for their able technical assistance. We appreciate the generosity of Dr. G. Nilaver, Department of Neurology, Columbia University college of Physicians and Surgeons, New York, NY 10032 (National Institutes of Health Grant HD-13147), and Dr. E. Lichtenstein, Department of Medicine, Yale-New Haven Hospital, New Haven, CT 06510, who supplied the somatostatin antiserum and Dr. S. E. Leeman, Department of Physiology, University of Massachusetts Medical Center, Worcester, MA 01605 (National Institutes of Health Grant AM 29876-02), and Dr. D. Landis, Department of Neurology, Massachusetts General Hospital, Boston, MA 02114, who allowed us to use their research facilities. We thank Dr. J. B. Martin for his thoughtful advice.

[2] To whom correspondence should be addressed at Department of Neurology, Warren 3, Massachusetts General Hospital, Fruit Street, Boston, MA 02114.

they may correspond. In this report, we present evidence at the light and electron microscopic levels that iSS is found within cells that have features similar to the medium size aspiny neurons which have been described in electron microscopic studies of Golgi impregnations (DiFiglia et al., 1980; Dimova et al., 1980) and intracellular labeled horseradish peroxidase (HRP) preparations (Bishop et al., 1982).

Materials and Methods

In three Sprague-Dawley rats (280 to 300 gm), tissue was fixed by intracardiac perfusion with 4% paraformaldehyde ($n = 1$) or with 4% paraformaldehyde containing 0.2% glutaraldehyde ($n = 2$). All fixatives were adjusted to pH 7.3 with buffer (0.15 M phosphate buffer). Colchicine (50 μg in 20 μl) was injected into the lateral ventricle 24 hr prior to perfusion with paraformaldehyde ($n = 1$) or paraformaldehyde with glutaraldehyde ($n = 1$). The peroxidase-antiperoxidase immunocytochemical method used in this laboratory for light and electron microscopy has been reported previously (Aronin et al., 1981). In brief, sections of 20- to 30-μm thickness were cut with a Vibratome (Lancer) and serially incubated in 0.2 M Tris/saline (TS; pH 7.6; 20 min), 3% normal goat serum in TS (30 min), SS antiserum (1:400 dilution; 18 to 36 hr at 4°C), TS with 1% goat serum (twice; 10 min), goat anti-rabbit IgG (1:20 dilution; 30 min), TS (twice; 10 min), and peroxidase-antiperoxidase complex (Miles; 1:30 dilution; 30 min). The sections then were treated with diaminobenzidine (0.013%) containing H_2O_2 (0.003%) for 6 to 10 min. Controls included tissue incubated with the SS antiserum preabsorbed with 20 μg/ml of synthetic SS (tetradecapeptide; Bachem, Inc.) or 20 μg/ml of synthetic SS_{28} (duodecapeptide; Peninsula, Inc.) or tissue not incubated in SS antiserum. The SS antiserum used in this study has been used previously (Feldman et al., 1979) and, by immunohistochemistry or radioimmunoassay, has no cross-reactivity with substance P, the enkephalins, vasopressin, or oxytocin (G. Nilaver and E. Lichenstein, personal communication).

For light microscopic review, sections were mounted onto glass slides with 0.5% gelatin. Sections for electron microscopy were taken from the glutaraldehyde-fixed tissue and were incubated in 2% osmium tetroxide (1 hr and 1% uranyl acetate (2 hr) and embedded in Epon supported by a plastic coverslip. Those regions with iSS labeling were cut into serial thin sections supported by Formvar-coated slot grids.

Results

Light microscopy. Immunoreactive SS cell bodies were observed in all regions of the caudate-putamen. Labeled neurons usually appeared singly. Occasionally, however, clusters of 3 to 5 iSS neurons also were found in all areas and they appeared more frequently in the ventral parts of the caudate. The total number of darkly labeled cells found in single coronal sections varied from 3 to 25 cells per section. Immunoreactive neurons did not appear to be more numerous in those animals treated with colchicine.

Positive neurons were of medium size (Figs. 1 to 5) and had round (9- to 15-μm), ovoid, pyramidal (both 12- to 16-μm in length), or fusiform (up to 20-μm in length) shapes. In some cells, the nuclei appeared clear and unlabeled (Fig. 5). Two to four labeled processes arose from each neuron and were observed to branch into secondary and tertiary processes which could be followed up to 120 μm from the cell body (Figs. 2 and 3). Emerging processes had either smooth or irregular contours which contained strictures (Fig. 2) and were of variable diameters (0.2 to 2 μm). Many of them appeared to curve as they coursed away from the cell body (Fig. 1). In addition, some processes were beaded (Figs. 3 and 5) or exhibited varicosities, the largest of which appeared at branch points (Fig. 4). Swellings were present on two or more processes and on thick as well as thin elements within the same neuron, suggesting that they belonged to dendrites as well as axons. Immunoreactive SS fibers also were found in the internal capsule bundles and throughout the caudate. Control sections in which the somatostatin antibody was preabsorbed with SS_{14} (Fig. 6) or SS_{28} failed to exhibit specific staining.

Electron microscopy. Ten iSS neurons from non-colchicine- ($n = 6$ neurons) and colchicine-treated ($n = 4$ neurons) rats were examined in serial sections at the electron microscopic level. The nuclei were usually devoid of peroxidase reaction product and, in all cases, exhibited indentations which were deep at some levels (Figs. 7, 8, and 11). Smaller rounded neurons showed a relatively thin rim of cytoplasm (Fig. 7) and larger ovoid or fusiform cells had more cytoplasm (Figs. 8 and 11). Peroxidase reaction product was deposited over the

Figures 1 to 5. Examples of immunoreactive SS neurons in the caudate nucleus of untreated (Figs. 1 to 4) and colchicine-treated (Fig. 5) rats using phase contrast photography.

Figure 1. An elongated neuron with four emerging processes which are of different diameters and which curve as they course away from the cell body. Note within each process the thicker (*arrows*) and thinner (*crossed arrows*) portions. *Scale bar*, 20 μm.

Figure 2. A neuron with two emerging dendrites, both of which give rise to thinner secondary branches. Note the constricted portions of one dendrite (*arrows*) and the enlargement at a branch point of another (*crossed arrow*). *Scale bar*, 20 μm.

Figure 3. A pyramidal shaped soma with three emerging processes, one of which bifurcates (*arrow*) into two fine beaded processes that are visible up to 80 μm from the cell body. *Scale bar*, 20 μm.

Figure 4. A rounded soma from which arises a dendrite with a large swelling (*arrow*) that branches into two thinner processes. One of the latter also exhibits a varicosity (*crossed arrow*). *Scale bar*, 20 μm.

Figure 5. An elongated iSS neuron in which the nucleus appears to be unlabeled. Three emerging processes of different diameters are visible and one gives rise to a fine beaded branch (*arrow*). *Scale bar*, 20 μm.

Figure 6. Preincubation control. Neurons in the caudate failed to exhibit specific staining for iSS when SS antibody was preabsorbed with SS_{14}. Phase contrast photography was used. *Scale bar*, 30 μm.

Figure 7. Ultrastructural features of an iSS neuron from a colchicine-treated rat. At this level, the nucleus, which is unlabeled, occupies a relatively large portion of the soma and has deep indentations (*arrows*). Strands of rough endoplasmic reticulum (RER) (*crossed arrow*) and a Golgi apparatus (*ringed arrow*) are present within the cytoplasm. *Scale bar*, 2 μm.

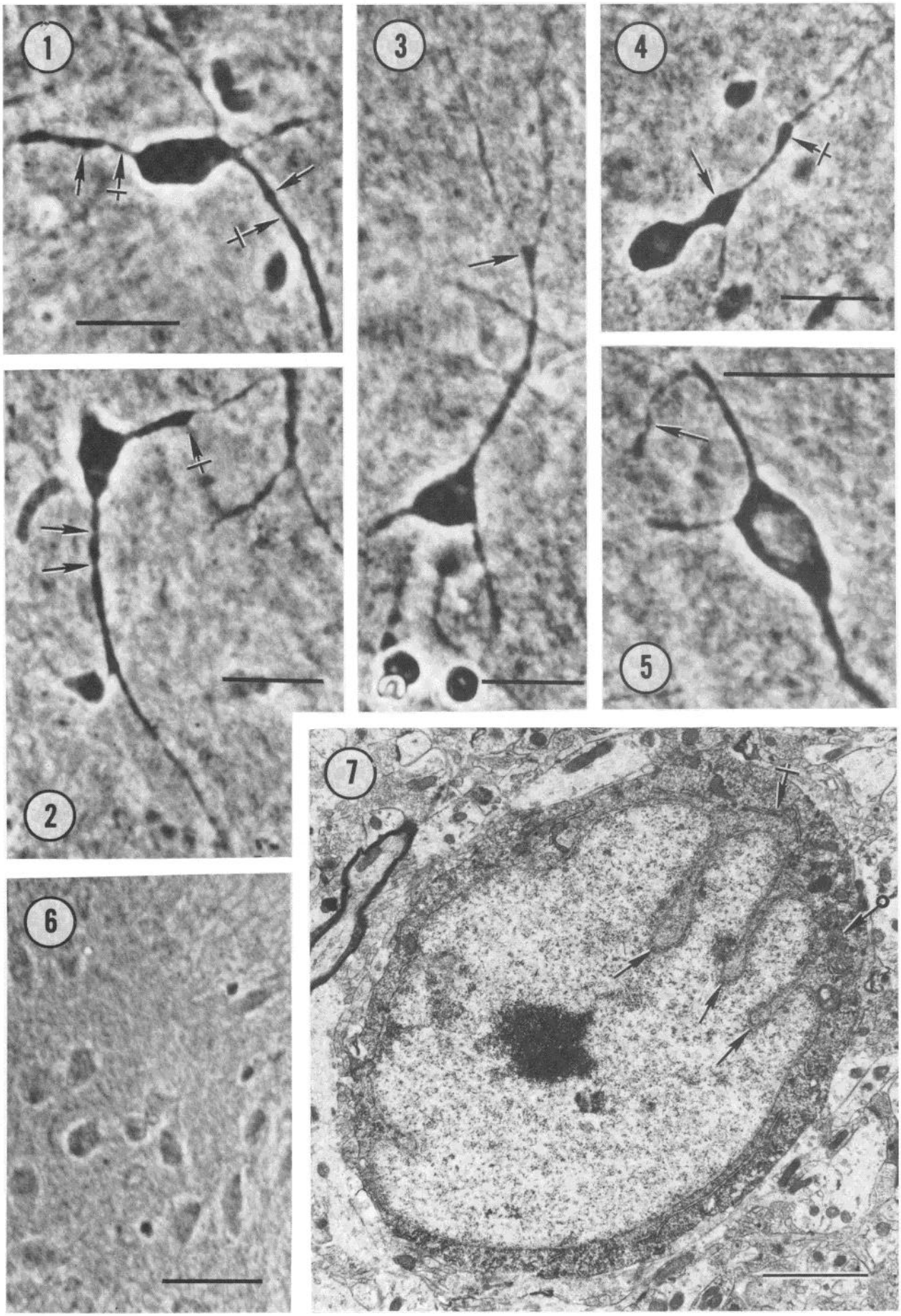
1
2
3
4
5
6
7

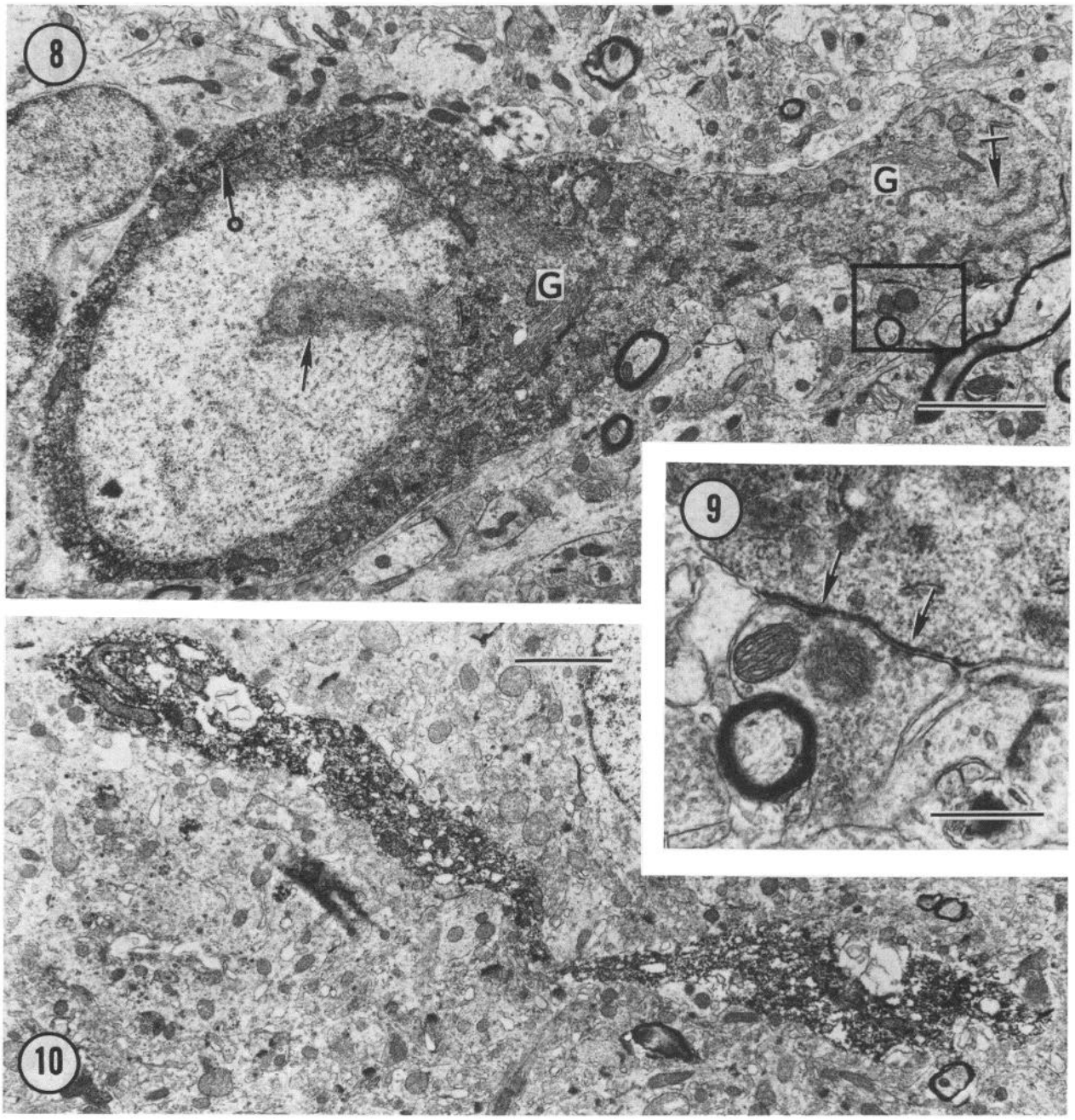

Figure 8. Somatostatin-containing neuron with an emerging dendrite in a colchicine-treated rat. The nucleus has a deep fold (*arrow*) and is surrounded by a rim of cytoplasm which contains y-shaped strands of RER (*ringed arrow*). A well developed Golgi apparatus (*G*) is present at the emergence of the dendrite. The latter, which is only lightly labeled, exhibits a swelling containing a Golgi apparatus (*G*) and stacks of RER (*crossed arrow*). The *region in the square* is shown in Figure 9. *Scale bar*, 2 μm.

Figure 9. Axodendritic synapse. The bouton contains numerous pleomorphic vesicles and forms a long synaptic contact (*arrows*) with the dendritic varicosity belonging to the neuron shown in Figure 8 (*inside square*). *Scale bar*, 0.5 μm.

Figure 10. Immunoreactive SS dendrite. This portion of the dendrite extended from 12 (*top left*) to 32 μm (*bottom right*) from an iSS soma and exhibits an irregular varicose appearance. Dendritic spines were not found in serial sections of the process. Colchicine was not used in this animal. *Scale bar*, 2 μm.

Figures 11 to 14. These are photographs of the same neuron which is from an untreated rat caudate.

Figure 11. Fusiform-shaped iSS soma with an emerging dendrite. The nucleus is elongated and is deeply enfolded (*arrows*). A stack of RER is present at one pole (*crossed arrow*). The dendrite is relatively thick, has irregular contours, and contains clusters of mitochondria and parallel arrays of microtubules. A synaptic contact is present in the *region in the square* which is shown in Figure 14. *Scale bar*, 2 μm.

Figure 12. Secondary dendrite of an iSS neuron. This portion of the dendrite, which was present 55 to 66 μm from its cell body (shown in Fig. 11), exhibits a varying diameter and contains parallel arrays of microtubules (*arrow*). A large granular vesicle is indicated by the *ringed arrow*. A round vesicle profile forms an asymmetric synapse at the *crossed arrow*. *Scale bar*, 1 μm.

Figure 13. Distal dendrite of an iSS neuron. This segment of the dendrite appeared about 70 to 78 μm from its cell body, which

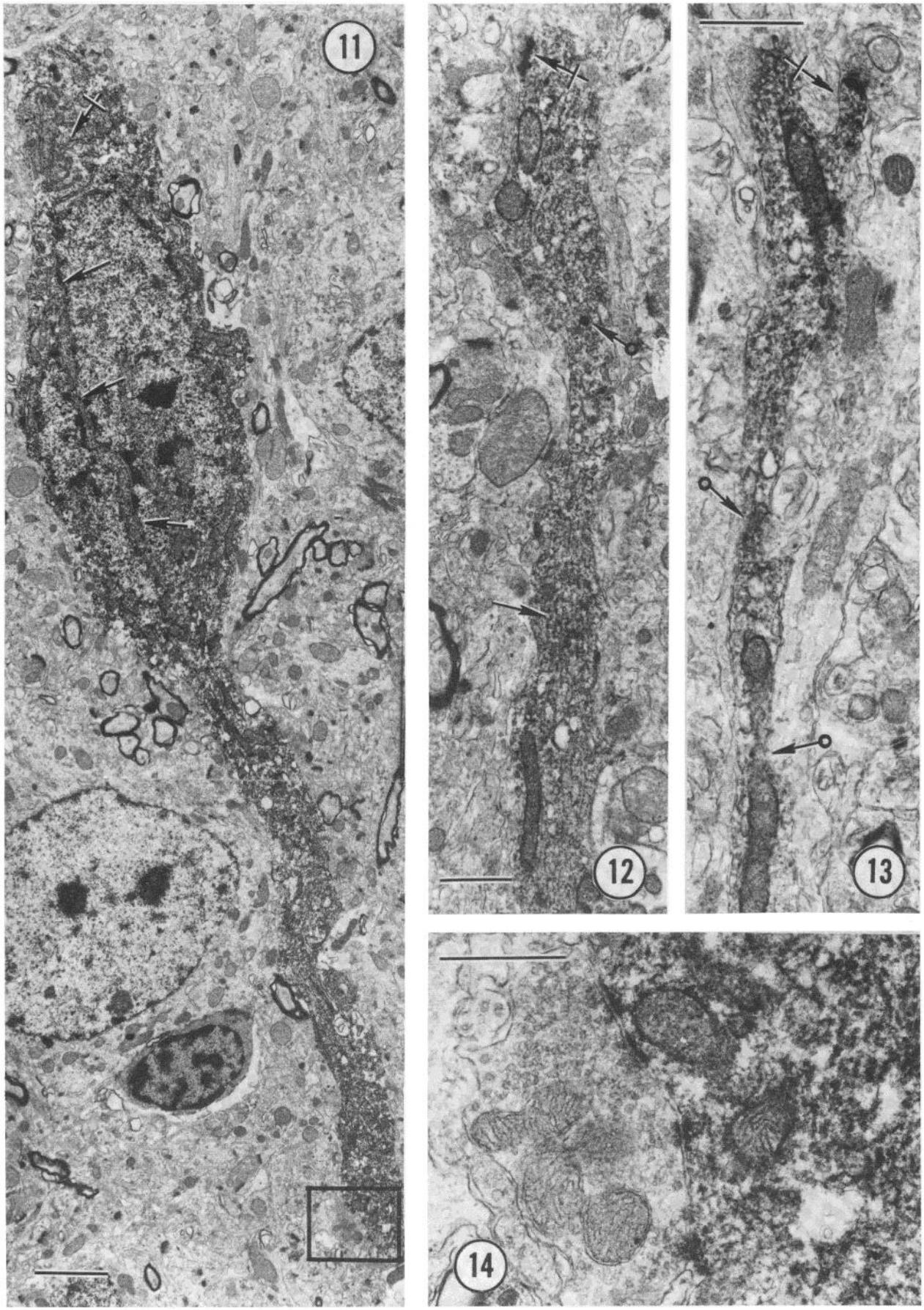

is shown in Figure 11, and was thought to belong to a tertiary branch. Note the constricted regions along the process (*ringed arrows*). A spine-like protrusion emerges at the *crossed arrow* and is postsynaptic to a round vesicle profile. *Scale bar*, 1 μm.

Figure 14. A synapse on a primary dendrite. A large bouton containing numerous pleomorphic vesicles makes multiple synaptic contacts with the dendrite of the iSS neuron shown in Figure 11 (*squared region*). *Scale bar*, 0.5 μm.

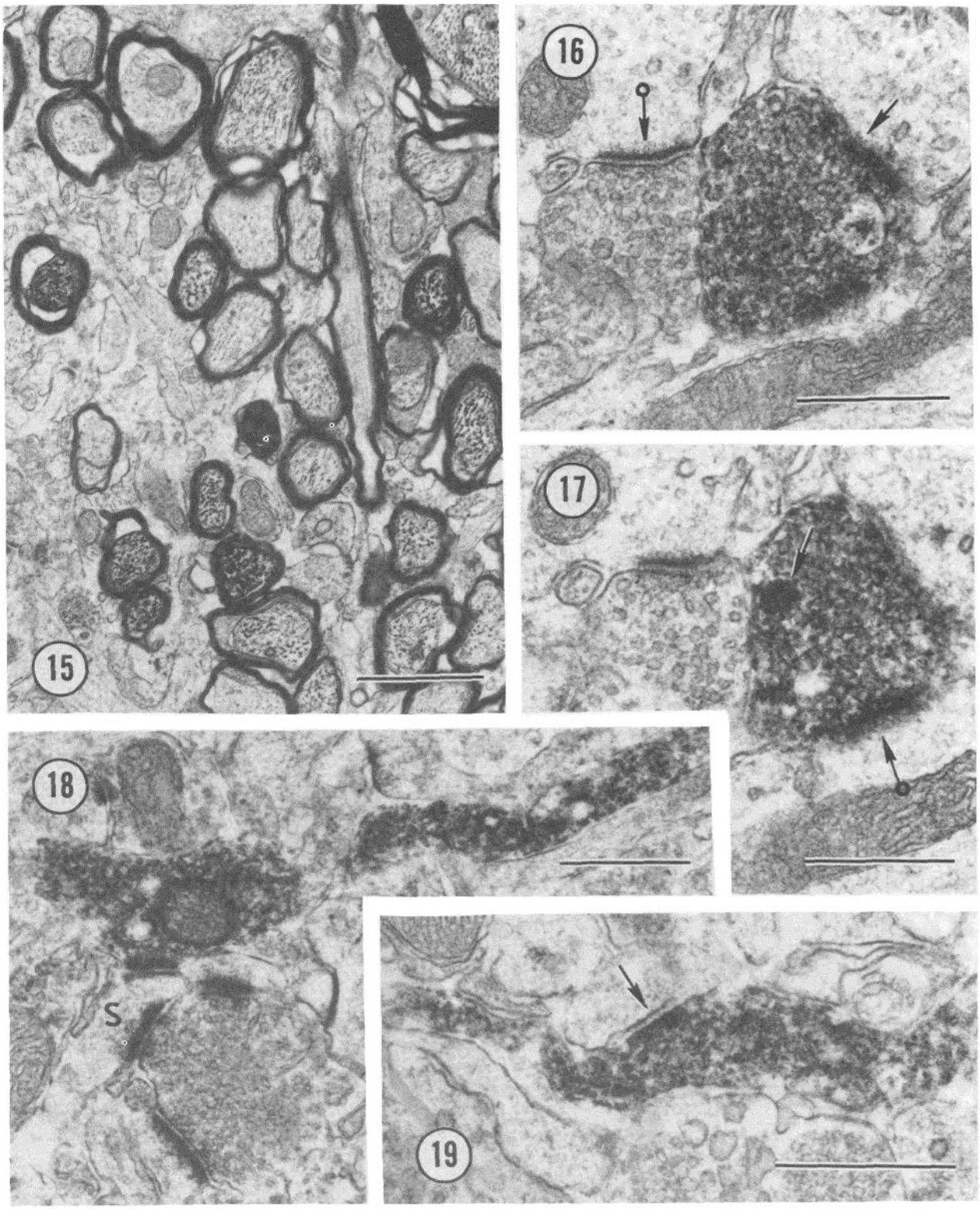

Figure 15. Immunoreactive SS myelinated axons. These labeled axons present in a bundle of internal capsule fibers are mostly of small diameter. *Scale bar*, 1 μm.

Figures 16 and 17. Serial sections of an iSS axon terminal. Figure 16 shows numerous clear pleomorphic vesicles on which peroxidase reaction produce is heavily deposited. A possible synapse with a dendrite is present at the *arrow*. Note the adjacent unlabeled bouton, also containing pleomorphic vesicles, which synapses with another dendrite (*ringed arrow*). *Scale bar*, 0.5 μm. In Figure 17, the same iSS terminal contains a large granular vesicle (*arrow*) and appears to make a synaptic contact with another dendrite (*ringed arrow*). *Scale bar*, 0.5 μm.

Figure 18. Axospinous synapse. An enlargement appears along a small diameter iSS axon, whose continuity was followed in serial sections, and synapses with a dendritic spine (*S*). The latter is also postsynaptic to an unlabeled axon terminal. *Scale bar*, 0.5 μm.

Figure 19. Synapse *en passant*. A small diameter iSS axon which is typical of those frequently observed in the caudate neuropil appears to contact a dendritic profile at the *arrow*. *Scale bar*, 0.5 μm.

membranes of most subcellular organelles. The latter included well developed Golgi apparatus (Figs. 7 and 8) and strands of rough endoplasmic reticulum (Fig. 7) which, in some cases, appeared as y-shaped structures (Fig. 8) or accumulated into small stacks (Nissl bodies; Fig. 11).

Eight of the neurons examined had emerging dendrites which contained peroxidase reaction product. The primary processes had either a uniform diameter along their course (Fig. 11) or a varicose appearance (Fig. 10). Most contained microtubules arranged in parallel arrays. Mitochondria, Golgi apparatus, and small stacks of rough endoplasmic reticulum also were observed (Fig. 8). In 2 of the neurons from the untreated rat, labeled secondary dendrites were followed up to 32 (Fig. 10) and 78 μm (Figs. 12 and 13) from their somata and exhibited irregular shapes and/or swellings. Only one spine-like protrusion was found in one of the dendrites (Fig. 13); it was located about 76 μm from the cell body and was postsynaptic to a small axon terminal. It should be noted that, in the neuropil, where labeled neurons and dendrites were present, dendritic spines were never observed to contain peroxidase reaction product.

Synaptic contacts onto iSS somata were observed infrequently. Those onto dendrites were more numerous and included at least two types of unlabeled axons. Profiles up to 1.5 μm in size with numerous pleomorphic vesicles (about 35 nm; Figs. 9 and 14) were seen to form synapses most frequently on proximal dendrites and boutons about 1.0 μm in size with many round vesicles (about 40 nm) which usually contacted distal branches (Figs. 12 and 13). Some of the round vesicle profiles were observed to contact both iSS dendrites and the spines of unlabeled dendrites.

Small diameter myelinated axons (0.2 to 0.5 μm) containing iSS were found in bundles of internal capsule fibers together with unlabeled axons (Fig. 15). In addition, very small diameter (0.1- to 0.2-μm) unmyelinated SS-positive fibers were seen coursing throughout the caudate neuropil. They formed swellings and made synapses *en passant* (Fig. 19). Immunoreactive SS axon terminals were relatively small in size (0.3 to 0.6 μm) and contained numerous pleomorphic vesicles (35 to 40 nm) on whose membranes peroxidase reaction product was heavily deposited (Figs. 16 and 17). Large granular vesicles (120 nm) were observed also in these profiles (Fig. 17). Labeled boutons synapsed with the shafts of dendrites (Figs. 16 and 17) and frequently with dendritic spines (Figs. 18 and 19). Most of the latter contacts had a short surface with symmetric membrane densities. Frequently, an iSS bouton contacted a dendritic spine which also was postsynaptic to an unlabeled axon terminal (Fig. 18).

Discussion

The present results confirm previous observations that iSS is contained within caudate cells of medium size (Graybiel et al., 1981). They also suggest that iSS neurons belong to the category of nonspinous or aspiny cells which have been described in Golgi studies in the rat (Mensah and Deadwyler, 1974; Lu and Brown, 1977), cat (Kemp and Powell, 1971), and monkey (Fox et al., 1971/72; DiFiglia et al., 1976), where they have been characterized by irregularly contoured and/or varicose dendrites containing few or no spines. Electron microscopic studies of Golgi-impregnated aspiny cells show that they have deeply indented nuclei and a relatively rich cytoplasm, including well developed Golgi apparatus and rough endoplasmic reticulum organized into stacks (DiFiglia et al., 1980, aspiny type I; Dimova et al., 1980, type III). Such ultrastructural features, which also resemble those recently identified in a medium aspiny neuron intracellularly labeled with HRP (Bishop et al., 1982), are very similar to those of iSS-containing cells found in the present study. Aspiny neurons have been observed infrequently in both the rat and cat (Mensah and Deadwyler, 1974; Kemp and Powell, 1971), which may account, in part, for the relatively sparse population of iSS somata observed in both species (Bennett-Clark et al., 1980; Graybiel et al., 1981). In the monkey, however, aspiny neurons have been observed more frequently (Pasik et al., 1979).

The morphologic features of iSS "aspiny" neurons contrast with those observed for medium spiny cells. The latter have numerous spines on portions of dendrite 20 μm or more from the cell body, few or no nuclear indentations, and a relatively scant cytoplasm (DiFiglia et al., 1980, spiny type I; Dimova et al., 1980, type I; Bishop et al., 1982, medium spiny). Electron microscopic immunocytochemical studies have shown that spiny neurons contain immunoreactive glutamic acid decarboxylase (GAD; Ribak et al., 1979) and enkephalins (Pickel et al., 1980; DiFiglia et al., 1982). Taken together, the above findings suggest that, in the neostriatum, iSS is contained within a population of neurons different from those which contain enkephalins and GAD. It is of interest that, in Huntington's disease, which is characterized by a loss of small and medium size neostriatal neurons (Bruyn et al., 1979), the concentration of iSS in the neostriatum is increased (Aronin et al., 1982). In contrast, the levels of γ-aminobutyric acid, enkephalin, and substance P, which are found in striatopallidal and striatonigral projections (Cuello and Paxinos, 1978; Hong et al., 1977; Jessel et al., 1978), have been shown to be reduced (Perry et al., 1973; Emson et al., 1980).

It is likely that many of the fine diameter fibers and small boutons found to contain iSS in the neostriatum belong to intrinsic iSS-containing somata. The axons of aspiny neurons in Golgi preparations have been observed to be thin, beaded processes which arborize locally (Kemp and Powell, 1971; Mensah and Deadwyler, 1974; Fox et al., 1971; DiFiglia et al., 1976). However, it is possible that some of the SS-positive axons are of extrinsic origin. The iSS myelinated fibers which were found within internal capsule bundles may belong, in part, to an incoming pathway. Somatostatin-containing cells are located in the cerebral cortex (Krisch and Leonhardt, 1980), which provides a major input to the caudate (Webster, 1961). A decrease in iSS concentrations of 50 to 70% in the neostriatum has been reported following mechanical lesions within the hypothalamus (Palkovits et al., 1980), a region which also contains numerous iSS neurons (Elde and Parsons, 1975). Whatever the origin of iSS labeled axons, their frequently observed synapses onto dendritic spines suggest that they interact in part with medium size spiny neurons. Somatostatin therefore

may have several roles in the neostriatum related to both intrinsic and afferent systems.

Finally, it is possible that some of the iSS neurons may have axons projecting to the globus pallidus since radioimmunoassayable iSS in the rat is reduced in the globus pallidus following kainate injection into the caudate (F. Beal and J. B. Martin, personal communication).

References

Aronin, N., M. DiFiglia, A. S. Liotta, and J. B. Martin (1981) Ultrastructural localization and biochemical features of immunoreactive Leu-enkephalin in monkey dorsal horn. J. Neurosci. *1:* 561–577.

Aronin, N., P. E. Cooper, L. J. Lorenz, S. M. Sagar, E. D. Bird, S. E. Leeman, and J. B. Martin (1982) Somatostatin is increased in the basal ganglia in Huntington's disease. Ann. Neurol., in press.

Bennett-Clark, C., M. A. Romagnano, and S. A. Joseph (1980) Distribution of somatostatin in the rat brain: Telencephalon and diencephalon. Brain Res. *188:* 473–486.

Bishop, G. A., H. T. Chang, and S. T. Kitai (1982) Morphologic and physiological properties of neostriatal neurons: An intracellular horseradish peroxidase study in the rat. Neuroscience *7:* 179–192.

Brownstein, M., A. Arimura, H. Sato, A. V. Schally, and J. S. Kizer (1975) The regional distribution of somatostatin in the rat brain. Endocrinology *96:* 1456–1461.

Bruyn, G. E., G. T. A. M. Bots, and R. Dom (1979) Huntington's chorea: Current neuropathological status. In *Huntington's Disease*, T. Chase, N. S. Wexler, and A. Barbeau, eds., pp. 83–93, Raven Press, New York.

Cuello, A. C., and G. Paxinos (1978) Evidence for a long leu-enkephalin strio-pallidal pathway in rat brain. Nature *271:* 178–180.

DiFiglia, M., P. Pasik, and T. Pasik (1976) A Golgi study of neuronal types in the neostriatum of monkeys. Brain Res. *114:* 245–256.

DiFiglia, M., T. Pasik, and P. Pasik (1980) Ultrastructure of Golgi-impregnated and gold-toned spiny and aspiny neurons in the monkey neostriatum. J. Neurocytol. *8:* 471–492.

DiFiglia, M., N. Aronin, and J. B. Martin (1982) Light and electron microscopic localization of immunoreactive leu-enkephalin in the monkey basal ganglia. J. Neurosci. *2:* 303–320.

Dimova, R., J. Vuillet, and R. Seite (1980) Study of the rat neostriatum using a combined Golgi-electron microscope technique and serial sections. Neuroscience *5:* 1581–1596.

Elde, R. P., and J. A. Parsons (1975) Immunocytochemical localization of somatostatin in cell bodies of the rat hypothalamus. Am. J. Anat. *144:* 541–548.

Elde, R., T. Hokfelt, O. Johansson, M. Schultzborg, S. Efendic, and R. Luft (1978) Cellular localization of somatostatin. Metabolism *27:* 1151–1159.

Emson, P. C., A. Arregui, V. Clement-Jones, B. E. B. Sandberg, and M. Rossor (1980) Regional distribution of methionine-enkephalin and substance P-like immunoreactivity in normal human brain and in Huntington's disease. Brain Res. *199:* 147–160.

Feldman, S. C., A. J. Silverman, and E. Lichtenstein (1979) Distribution of somatostatin-containing neurons in the guinea pig forebrain. Soc. Neurosci. Abstr. *5:* 526.

Finley, J. C. W., J. L. Maderdrut, L. J. Roger, and P. Petrusz (1981) The immunocytochemical localization of somatostatin-containing neurons in the rat central nervous system. Neuroscience *6:* 2173–2192.

Fox, C. A., A. N. Andrade, R. C. Schwyn, and J. A. Rafols (1971/72) The aspiny neurons and the glia in the primate striatum: A Golgi and electron microscopic study. J. Hirnforsch. *13:* 341–362.

Graybiel, A. M., C. W. Ragsdale, Jr., E. S. Yoneaka, and R. P. Elde (1981) An immunohistochemical study of enkephalins and other neuropeptides in the striatum of the cat with evidence that the opiate peptides are arranged to form mosaic patterns in register with the striosomal compartments visible by acetylcholinesterase staining. Neuroscience *6:* 377–398.

Hong, J. S., H. Y. Yang, G. Racagni, and E. Costa (1977) Projections of substance P containing neurons from neostriatum to substantia nigra. Brain Res. *122:* 541–544.

Jessel, T. M., P. C. Emson, G. Paxinos, and A. C. Cuello (1978) Topographic projections of substance P and GABA pathways in the striato- and pallido-nigral-system: A biochemical and immunohistochemical study. Brain Res. *152:* 487–498.

Kemp, J. M., and T. P. S. Powell (1971) The structure of caudate nucleus of the cat: Light and electron microscopy. Philos. Trans. R. Soc. Lond. (Biol.) *262:* 328–401.

Kobayashi, R. M., M. Brown, and W. Vale (1977) Regional distribution of neurotensin and somatostatin in rat brain. Brain Res. *126:* 584–588.

Krisch, B. (1978) Hypothalamic and extrahypothalamic distribution of somatostatin-immunoreactive elements in the rat brain. Cell Tissue Res. *195:* 499–513.

Krisch, B., and H. Leonhardt (1980) An intermittent somatostatin-immunoreactivity in the cortex and basal ganglia of the rat. Cell Tissue Res. *205:* 327–331.

Lu, E. J., and W. J. Brown (1977) The developing caudate nucleus in the euthyroid and hypothyroid rat. J. Comp. Neurol. *171:* 261–284.

Mensah, P., and S. Deadwyler (1974) The caudate nucleus of the rat: Cell types and the demonstration of a commissural system. J. Anat. *117:* 281–293.

Palkovits, M., R. M. Kobayashi, M. Brown, and W. Vale (1980) Changes in hypothalamic, limbic and extrapyramidal somatostatin levels following various hypothalamic transections in rat. Brain Res. *195:* 499–505.

Pasik, P., T. Pasik, and M. DiFiglia (1979) The internal organization of the neostriatum in mammals. In *The Neostriatum*, I. Divac and R. G. E. Oberg, eds., pp. 5–36, Pergamon Press, Oxford.

Perry, T. L., S. Hansen, and M. Kloster (1973) Huntington's chorea: Deficiency of γ-aminobutyric acid in brain. N. Engl. J. Med. *288:* 337–342.

Pickel, V. M., K. K. Sumai, S. C. Beady, R. J. Miller, and D. J. Reis (1980) Immunocytochemical localization of enkephalin in the neostriatum of rat brain: A light and electron microscopic study. J. Comp. Neurol. *189:* 721–740.

Ribak, C. E., J. E. Vaughn, and E. Roberts (1979) The GABA neurons and their axon terminals in rat corpus striatum as demonstrated by GAD immunocytochemistry. J. Comp. Neurol. *187:* 261–284.

Webster, K. E. (1961) Cortico-striate interrelations in the albino rat. J. Anat. *95:* 532–544.